

# Improved Temporal Stability of the Second-Order Nonlinear Optical Effect in a Sol–Gel Matrix Bearing an Active Chromophore

Dong Hoon Choi,<sup>\*,†</sup> Ji Hye Park,<sup>†</sup> Tae Hyung Rhee,<sup>‡</sup> Nakjoong Kim,<sup>§</sup> and Sin-Doo Lee<sup>⊥</sup>

Department of Textile Engineering, Division of Material Science & Technology, I.L.R.I., Kyung Hee University, Yongin-shi, Kyungki-Do 449-701, Korea; Telecom. R&D Center, Samsung Electronics Co., Ltd., Suwon P.O. Box 105, Kyungki-Do, 440-600 Korea; Division of Polymer Research, Korea Institute of Science and Technology, Cheongryang P.O. Box 131, Seoul, 130-650 Korea; and School of Electrical Engineering, Seoul National University, 151-742 Korea

Received May 2, 1997. Revised Manuscript Received November 24, 1997

A second-order nonlinear optical (NLO) chromophore (disperse red 1) was reacted with (3-isocyanatopropyl)triethoxysilane to form a functionalized silicon alkoxide precursor (SGDR1). To improve the temporal stability of the second-order NLO effect, we employed a thermal cross-link between the organic side groups themselves. (3-Glycidoxypropyl)-trimethoxysilane was mixed with SGDR1 in tetrahydrofuran (SGDR1/GPTS). We compared the temporal stability of the poled samples with SGDR1 and SGDR1/GPTS. We investigated second-order NLO properties of sol–gel films by virtue of second harmonic generation (SHG) and linear electrooptic (E/O) coefficient measurements for the purpose. We achieved much improvement in the temporal stability of second-order NLO effect at high temperature with the heterogeneous films.

## Introduction

Organic and inorganic hybrid materials through sol–gel processes have been highlighted for photonic applications in recent years.<sup>1–3</sup> Sol–gel processes with silicon alkoxides can form various microstructures easily.<sup>4,5</sup> Silicon alkoxide can be hydrolyzed in the presence of water and a catalytic amount of acid. Transparent films can be fabricated after hydrolysis and partial condensation of the solution. Silicon trialkoxide can be designed to bear a functional chromophore in one arm of silicon through a flexible spacer. The resultant structure is similar to that of a side-chain NLO polymer.

Second-order NLO properties of poled polymers have been extensively studied for over a decade.<sup>6–10</sup> One difficulty for poled organic polymer arose from the poor

thermal and temporal stability of the NLO activity at high temperature. Among the other requirements for practical applications, the important issue with poled polymers is postulated that the temporal stability of the dipolar alignment should be much improved. For this purpose, we made attempts to prepare the cross-linked silylated films.<sup>11–13</sup> The covalent bond of the chromophore to the silicon network can give us higher concentrations of the NLO unit in the matrix. The solution of SGDR1 is subjected to hydrolysis and condensation. Curing the film at high temperature (>200 °C) leads to densification of the silicon oxide matrix but results in partial decomposition of the organic NLO chromophore. Moreover, the temporal stability of the NLO effect at high temperature is significantly worse than that of the poled organic polymer.

In attempts to improve both second-order NLO effect and its temporal stability, we designed the sol–gel precursor in such a way finally that a high concentration of chromophore was obtained. Heterogeneous mixed solutions of SGDR1 and GPTS were used for the purpose. Second-order NLO properties of prepared sol–gel films were investigated by second harmonic generation (SHG) and linear electrooptic coefficient measure-

<sup>†</sup> Kyung Hee University.

<sup>‡</sup> Samsung Electronics Co., Ltd.

<sup>§</sup> Korea Institute of Science and Technology.

<sup>⊥</sup> Seoul National University.

(1) Chaput, F.; Riehl, D.; Levy, Y.; Boilot, J.-P. *Chem. Mater.* **1993**, *5*, 589.

(2) Kim, J. S.; Plawsky, J. L.; LaPerute, R.; Korenowski, G. M. *Chem. Mater.* **1992**, *4*, 249.

(3) Jeng, R. J.; Chen, Y. M.; Chen, J. I.; Kumar, J.; Tripathy, S. K. *Macromolecules* **1993**, *26*, 2530.

(4) Harvy, Y.; Webber, S. E. *Chem. Mater.* **1991**, *3*, 501.

(5) Avnir, D.; Kaufmann, V. R.; Reissfeld, R. *J. Non-Cryst. Solids* **1985**, *74*, 395.

(6) Pretre, Ph.; Kaatz, P. G.; Meier, U.; Günter, P.; Zysset, B.; Ahleim, M.; Stahelin, M.; Lehr, F. *Polym. Prepr.* **1994**, *35*, 136.

(7) Michelotti, F.; Toussare, E.; Levenson, R.; Liang, J.; Zyss, J. *Appl. Phys. Lett.* **1995**, *67*, 2765.

(8) Ye, C.; Mark, T. J.; Yang, J.; Wong, G. K. *Macromolecules* **1987**, *20*, 2322.

(9) Choi, D. H.; Kim, H. M.; Wijekoon, W. P. K. M.; Prasad, P. N. *Chem. Mater.* **1992**, *4*, 1253.

(10) Stahelin, M.; Zysset, B.; Ahlheim, M.; Marder, S. R.; Bedworth, P. V.; Runser, C.; Barzoukas, M.; Fort, A. *J. Opt. Soc. Am. B* **1996**, *13*, 2401.

(11) Levenson, R.; Liang, J.; Zyss, J. *Polym. Prepr.* **1994**, *35*, 162.

(12) Shi, Y.; Olson, D. J.; Bechtel, J. H.; Kalluri, S.; Steier, W. H.; Wang, W.; Chen, D.; Fetterman, H. R. *Appl. Phys. Lett.* **1996**, *68*, 1040.

(13) Ho, M. S.; Barrett, C.; Paterson, J.; Esteghamatian, M.; Natansohn, A.; Rochon, P. *Macromolecules* **1996**, *29*, 4613.

ments. We investigated the difference in the temporal stability between the homogeneous (SGDR1) and heterogeneous (SGDR1/GPTS) films. The formation of a cross-link between the epoxy and urethane groups in GPTS and SGDR1 was investigated by in situ IR spectral analysis. We confirmed the improvement of temporal stability by in situ SHG measurement and also monitored the decay of electrooptic coefficient ( $r_{33}$ ) at high temperatures.

### Experimental Section

**Materials.** (3-Isocyanatopropyl)triethoxysilane, dibutyltin dilaurate (DBTDL), and (3-glycidoxypropyl)trimethoxysilane (GPTS) were purchased from Aldrich Chemical Co. and used without further purification. Disperse red 1 was recrystallized from ethanol.

**Synthesis.** We dissolved (3-isocyanatopropyltriethoxy)silane (2.0 g, 8.08 mmole) and disperse red 1 (DR1, 1.27 g, 4.04 mmol) in freshly dried tetrahydrofuran (THF, 30 mL). The solution was refluxed for 4 h with a catalytic amount of dibutyltin dilaurate (DBTDL). The solution was concentrated and added into hexane to get a red precipitate. The resultant product (SGDR1) was dried at 60 °C for 24 h and stored in a desiccator saturated by argon; yield 80%.

$^1\text{H}$  NMR (DMSO- $d_6$ )  $\delta$ (ppm) 8.25 (d, 2H), 7.83 (d, 2H), 7.75 (d, 2H), 6.72 (d, 2H), 5.07 (t, 1H), 4.22 (t, 2H), 3.78 (q, 6H), 3.65 (t, 2H), 3.51 (q, 2H), 3.08 (q, 2H), 1.60 (m, 2H), 1.22 (m, 12H), 0.58 (t, 2H). FT IR: NH stretching 3329  $\text{cm}^{-1}$  (hydrogen bonded), 3420  $\text{cm}^{-1}$  (isolated) carbonyl (C=O) 1698  $\text{cm}^{-1}$  (hydrogen bonded), 1725  $\text{cm}^{-1}$  (isolated)  $\text{NO}_2$  1516  $\text{cm}^{-1}$ .

**Materials Processing.** The red solid (SGDR1, 1 mol) was dissolved in THF. Water (4 mol) and 0.02–0.04 mol of hydrochloric acid (HCl) was added to the solution. The solution was hydrolyzed and aged at room temperature for 48 h. The solution for the heterogeneous film was prepared by mixing SGDR1 with GPTS (50 mol %). The solutions were spin coated on the polished KBr windows for the in situ infrared spectroscopic study. For studying the NLO effect, thin films were fabricated on indium tin oxide (ITO) precoated glass and ordinary normal microslide glass by using a filtered solution. We measured the thickness of the film using Tencor P10. The refractive index and thickness of the film coated on silicon wafer were measured with a Metricon instrument simultaneously at three different wavelengths (632, 1300, and 1550 nm).

For second harmonic generation (SHG) experiments, we poled the films using a corona poling technique in a wire-to-plane geometry.<sup>14,15</sup> For linear electrooptic coefficient measurement, we deposited the gold electrode on top of the film to fabricate sandwiched samples.

**Second Harmonic Generation (SHG).** In situ second harmonic generation (SHG) measurements of samples were carried out with a Q-switched mode-locked  $\text{Nd}^{3+}$ :YAG laser operating in the TEM<sub>00</sub> mode. The samples were mounted on the hot stage and corona poled. We integrated the second harmonic (SH) signals during poling for optimizing the poling conditions. For calculation of the absolute value of the second-order NLO coefficient,  $d_{33}$ , we followed the standard Maker fringe technique that was already well described.<sup>16</sup> Assuming the Kleinman's symmetry rule, we used the p-p fringe to calculate the  $d_{33}$  value. The SH signal was normalized with respect to that of a calibrated quartz crystal (Y-cut) whose  $d_{11}$  is 0.5 pm/V.<sup>17</sup>

**Electrooptic Coefficient Measurement.** We measured the linear electrooptic coefficients of the samples by way of

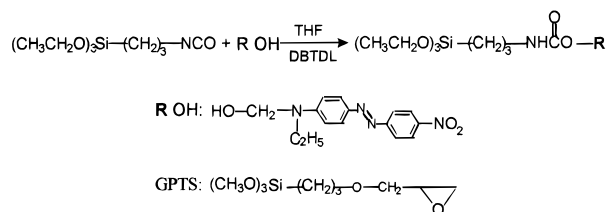


**Figure 1.** Synthetic scheme for NLO-active silane and the structure of GPTS.

reflection technique which is based on the difference of phase retardation in TE and TM mode.<sup>18,19</sup> Wavelengths of 632, 830, and 1300 nm were used for this measurement. The sine wave voltage (10  $V_{\text{rms}}$  at 1 kHz) was applied to each sample during recording the modulated signal. The linear electrooptic coefficient " $r_{33}$ " was calculated by the following equation:

$$r_{33} = \frac{3\lambda I_m}{4\pi V_m I_c n^2} \frac{(n^2 - \sin^2 \theta)^{1/2}}{\sin^2 \theta} \quad (1)$$

where  $I_m$  is the amplitude of the electrooptic modulation,  $V_m$  is the ac voltage applied to the sample, and  $I_c$  is the intensity of the incident light where phase retardation is 90° between the TE and TM modes.

### Results and Discussion

We prepared the NLO-active triethoxysilane by a simple urethane forming reaction between alcohol and isocyanate.<sup>20</sup> The synthetic scheme is illustrated in Figure 1. The product is well soluble in THF, acetone, dimethylformamide, pyridine, etc. In this study, we selected THF as a solvent for the sol-gel process.

**1. Infrared Spectral Analysis of SGDR1.** We deposited thin films on a KBr window via spin coating for in situ IR spectral analysis. The IR spectrum shows the existence of hydrogen bonds between the organic side chains at room temperature. We could observe superposed bands at 1698 and 1725  $\text{cm}^{-1}$  in the IR spectra of SGDR1 films. We assigned those two bands to hydrogen-bonded and isolated carbonyl stretching vibrations in carbamate, respectively. Simultaneously, another overlapped bands could be observed at 3329 and 3420  $\text{cm}^{-1}$ , which were similarly assigned to hydrogen-bonded and isolated NH stretching vibration modes. Thus, it is apparent that the inter- or intramolecular hydrogen-bonds exist between the carbamate groups in the SGDR 1 matrix. The fraction of hydrogen-bonded carbonyl group was calculated around 0.862 at 25 °C by analyzing the peak fitted to Gaussian function. The fraction of isolated carbonyl groups increased gradually with heating (see Figure 2). During cooling, the hydrogen bonds were regenerated slowly. The fraction of hydrogen-bonded carbonyl group was found to be 0.852 after cooling the sample at 25 °C. We also could see the same tendency in NH stretching band around 3420–3329  $\text{cm}^{-1}$ . Therefore, the formation of hydrogen bonds was found to be thermally *quasi-reversible* in SGDR1 matrix.

**2. Second-Order NLO Effect of SGDR1.** *2.1. Decaying Behavior of  $r_{33}$  of SGDR1.* We fabricated the

(14) Mortazavi, M. A.; Knoesen, A.; Kowel, S. J. *J. Opt. Soc. Am. B* **1989**, *6*, 733.

(15) Wijekoon, W. M. K. P.; Zhang, Y.; Karna, S. P.; Prasad, P. N.; Griffin, A. C.; Bhatti, A. M. *J. Opt. Soc. Am. B* **1992**, *9*, 1832.

(16) Singer, K. D.; Sohn, J. E.; Lalama, S. J. *Appl. Phys. Lett.* **1986**, *49*, 248.

(17) Jerphagnon, J.; Kurtz, S. K. *Phys. Rev. B* **1970**, *1*, 1739.

(18) Teng, C. C.; Mann, H. T. *Appl. Phys. Lett.* **1990**, *56*, 30.

(19) Shuto, Y.; Amano, M. *J. Appl. Phys.* **1995**, *77*, 4632.

(20) Choi, D. H.; Lim, S. J.; Jahng, W.S.; Kim, N. *Thin Solid Films* **1996**, *287*, 220.

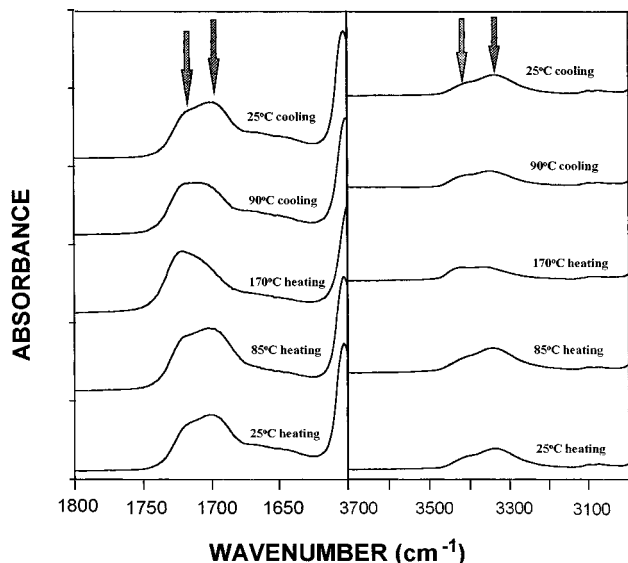


**Figure 2.** Infrared spectra of SGDR1 with the heating and cooling cycle.

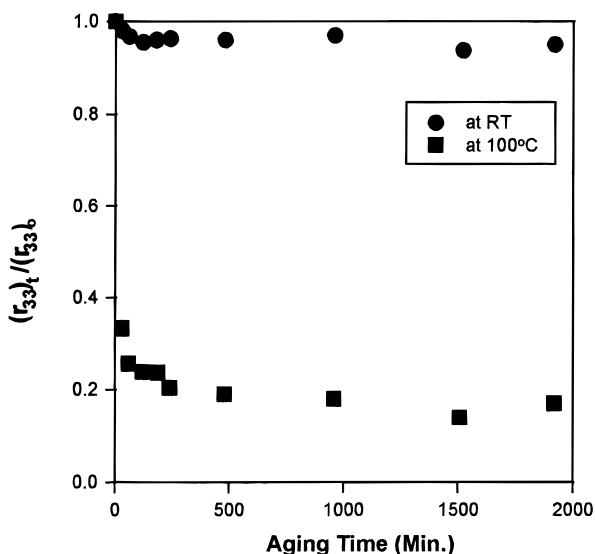


**Figure 3.** Decaying behavior of  $I_{33}$  of SGDR1 at room temperature and 100 °C.

E/O sandwiched samples with SGDR1 between ITO and gold electrode. The samples were poled and annealed for 2 h. Initially, the film was dried under argon and poled at 100 °C for 1 h. The temperature was raised to 200 °C, and the sample was annealed for another 1 h. We observed the decaying behaviors of the E/O effect after aging the samples at 25 and 100 °C. At room temperature, the E/O coefficient was sustained to 90–95% of the initial value. However, the coefficient fell to ~25% of the initial one after annealing at 100 °C only for 30 min. After 30 h at 100 °C, only 15–17% of the initial signal remained (see Figure 3). We could fit the decaying curves to double exponential function,  $A \exp(-t/\tau_1) + (1 - A)\exp(-t/\tau_2)$ . Two-step relaxations were analyzed in terms of relaxation times,  $\tau_1$  and  $\tau_2$ . We could calculate  $\tau_1$  and  $\tau_2$  to be 16.2 and 3974 min, respectively.

We considered that decay of the NLO effect could partially be ascribed to the collapse of the hydrogen bond between side groups in the first stage. The hydrogen bonds start to be disorganized around 90–

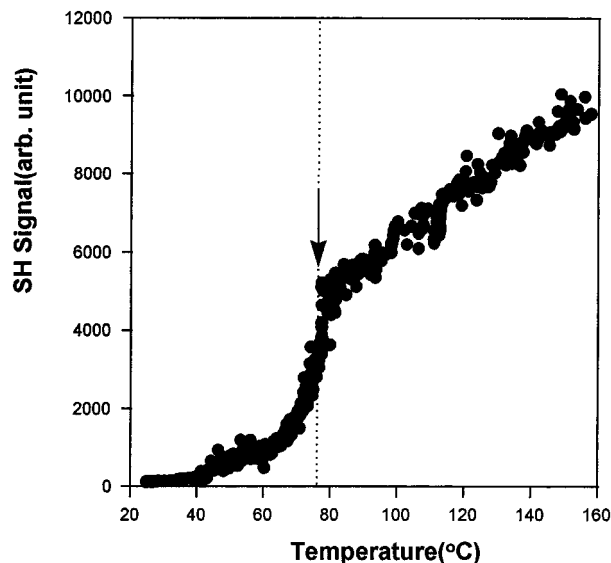


**Figure 4.** Temperature dependence of SH signal of SGDR1.

100 °C. As we observed in the IR spectra, the hydrogen bond between the secondary amine and the carbonyl group was affected thermally. If the density of silicon oxide in the matrix is identical, the other factor to affect decaying behavior is the decrease in the density of the hydrogen bond. This suggestion was supported by the results of in situ SHG experiments.

**2.2. Second Harmonic Generation (SHG): Decay of  $d_{33}$  at 100 and 150 °C.** With the results in the electrooptic study, we traced the second harmonic (SH) signal during poling. The SH signal increased slowly from 40 °C and fast around 80–90 °C. Usually, the NLO side-chain polymer could not be poled at that low temperature. However, SH signal could be observed while applying the electric field at low temperature, because the pristine film consisted of very low molecular weight oligomers. Condensation between silicon hydroxide did not proceed enough to form a highly organized silicon oxide network. The matrix did not show any polymeric behavior in the thermal transition, i.e., did not exhibit glass transition behavior in DSC thermogram. Around 75–80 °C, the SH signal starts to increase rapidly. This temperature coincided roughly with the temperature at which hydrogen bonds start to be broken as was found during in situ IR spectral analysis (see Figure 4).

We poled the sample under 4.5 kV of corona field at 100 °C for 1 h and annealed it at 200 °C for 1 h. We placed the poled sample on the corona poling stage and applied the electric field at room temperature. The incident angle of the laser was set at 48° to the surface of the film. Then, we raised the temperature to 100 °C. After this reached 100 °C, we turned off the voltage to observe the decay of the SH signal. The signal fell down to 10% of initial one within 30 min (see Figure 5). After the voltage was turned on again, the signal recovered to the same value as that measured before turning off the applied field. Under the same method as above, we traced the decaying behavior of the SH signal at 150 °C. The signal approached closely to zero within 10 min (see Figure 5). These results indicate that SGDR1 shows a significantly poor temporal stability of the second-order NLO effect at 100 and 150 °C.

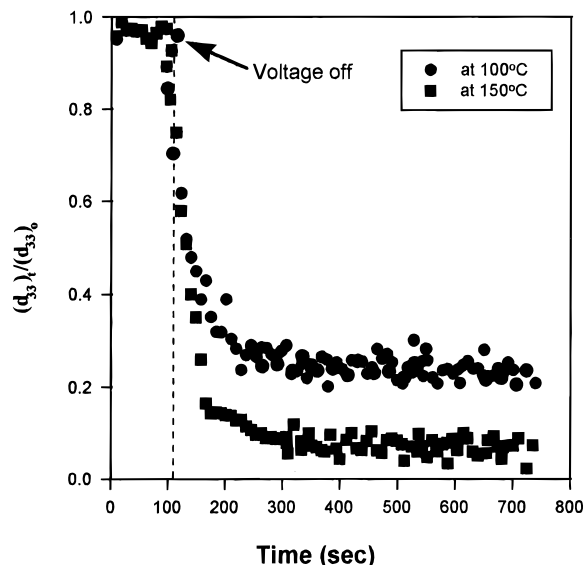


**Figure 5.** Decaying behavior of SH signal of SGDR1 at 100 and 150 °C.

**3. IR Spectral Analysis of Heterogeneous Film (SGDR1/GPTS).** During thermal condensation of SGDR1 at 200–210 °C for a long time, an appreciable portion of the chromophore decomposed. The optical quality of the film turned was poor. To avoid this severe thermal condition, we made an effort to induce a thermal cross-link besides the silicon oxide network at well below 200 °C. In principle, the lone pair of electrons in secondary amine can attack the less crowded carbon in the epoxide to open a ring. In this conversion, tertiary amine can be formed after partial consumption of secondary amine. In situ IR spectroscopy could give us requisite information about how the internal structure changed. With an increase in annealing temperature, hydrogen bonds were broken gradually, similar to SGDR1. After raising the temperature to 150–160 °C, a new carbonyl band started to appear around 1745  $\text{cm}^{-1}$ . At the same time, the absorbance of the secondary amine decreased at 3420  $\text{cm}^{-1}$ . The force constant of the carbonyl double bond near the tertiary amine group may be higher than that of carbonyl in the original carbamate (see Figure 6). The high force constant and definite double-bond character of the carbonyl group can drive to form a new band at the higher wavenumber of 1745  $\text{cm}^{-1}$ . Then, we cooled the sample to room temperature again. Compared to the previous homogeneous SGDR1, we could observe *irreversibility* of the hydrogen bond in the heterogeneous film. This implies that the cross-link reaction proceeded to some extent during annealing so that the molecular interaction was partially limited.

In the IR spectrum of a pristine SGDR1/GPTS film, the trace of the epoxide band (appeared at 906  $\text{cm}^{-1}$ ) almost disappeared after thermal treatment at 160–170 °C for 30–100 min (see Figure 6). In short, we confirmed some extent of the cross-link in the organic parts accompanying densification of silicon oxide network. We could impart two different kinds of a densification process in one matrix.

#### 4. Second-Order NLO Effect of SGDR1/GPTS.

**4.1. Decaying Behavior of  $r_{33}$  of Heterogeneous Film (SGDR1/GPTS).** We could improve the temporal sta-

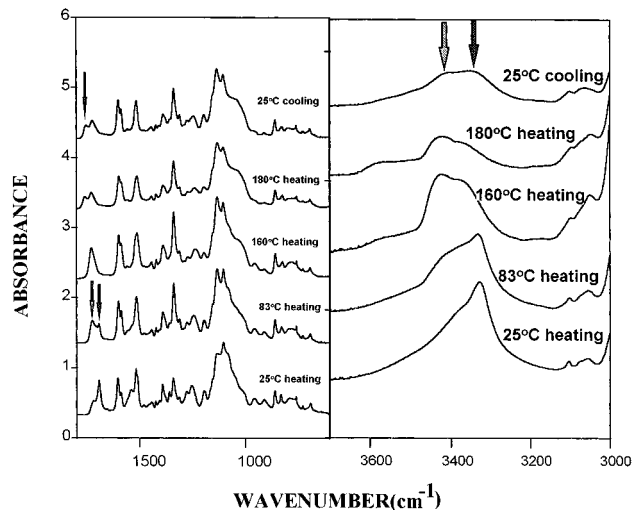


**Figure 6.** Infrared spectra of SGDR1/GPTS with heating and cooling cycle.

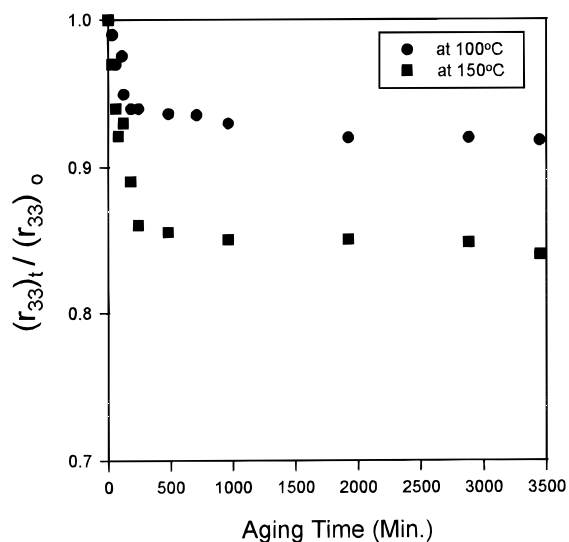


**Figure 7.** Decaying behavior of  $r_{33}$  of SGDR1/GPTS at 100 and 150 °C.

bility much after poling and curing using the heterogeneous film. We poled the sample at 100 °C under 50  $\text{V}/\mu\text{m}$  for 30 min and cured it at 170 °C for 1 h in the presence of an electric field. While aging at 100 °C for 30 min, slight decay of the electrooptic effect was observed. 80–85% of the initial electrooptic signal remained at 150 °C even after annealing for 50 min (see Figure 7). The results of IR analysis showed that when the film was stored at 150 °C or higher, cross-linking took place to some extent. This helped to reduce the decrement of the initial E/O coefficient even after storing them at 100 or 150 °C. The relaxation curve at each temperature was analyzed in terms of the relaxation times,  $\tau_1$ , and  $\tau_2$  which are shown in Table 1. Considering the calculated relaxation times, we can expect the long-term stability of the device that can be fabricated with this matrix.

**4.2. Second Harmonic Generation (SHG): Decaying of  $d_{33}$  of the Heterogeneous Film at 100 and 150 °C.** We traced the SH signal during poling using the SGDR1/GPTS film. The signal increased gradually from 40 °C, and the rate of increase became relatively larger around 90–100 °C. This temperature range is also consistent

**Table 1. Measured and Calculated Values for SGDR1 and SGDR1/GPTS**

|            | $r_{33}$ (pm/V) <sup>a</sup> |        |         | $d_{33}$ (pm/V) <sup>b</sup><br>at 1064 nm | decaying behavior of $r_{33}$ |                |                |         |
|------------|------------------------------|--------|---------|--|-------------------------------|----------------|----------------|---------|
|            | 632 nm                       | 830 nm | 1300 nm |  | A                             | $\tau_1$ (min) | $\tau_2$ (min) |         |
| SGDR1      | 65.5                         | 14.3   | 10.8    | 54.0                                       | 100 °C                        | 0.782          | 16.2           | 3974    |
| SGDR1/GPTS | 54.0                         | 9.0    | 8.2     | 42.7                                       | 100 °C                        | 0.068          | 89.1           | 150 138 |
|            |                              |        |         |  | 150 °C                        | 0.173          | 178.9          | 41 934  |

<sup>a</sup> The samples were poled under 50 V/ $\mu$ m; electrode poling. <sup>b</sup> The samples were corona poled under 4.5 kV.

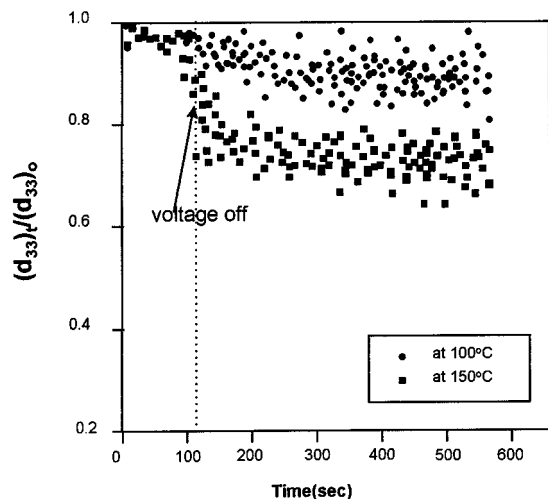


**Figure 8.** Decaying behavior of SH signal of SGDR1/GPTS at 100 and 150 °C.

with the temperature at which hydrogen bonds were disrupted. To observe the decaying behavior of the SH signal, we corona poled the sample under 4.5 kV for 1 h and cured at 170 °C for 1 h. We did the same experiment as we did using SGDR1. First, after annealing at 100 °C, the SH signal was maintained at almost 85–90% even after 10 min in the absence of the corona field (see Figure 8). After annealing at 150 °C for 9 min, the SH signal was decayed to 70–75% of the initial value. After tracing the decaying behavior of SH

signal, we raised the temperature at 180 °C to pole the sample again. We applied a higher electric field, 5 kV, than that we initially applied. No increment of the SH signal was observed. This indicates that the cross-linked structure started to form partially at 170 °C, imparting some rigidity to the organic side groups.

We are making efforts to optimize the poling time and temperature in order not to deteriorate the optical quality of the sol–gel heterogeneous film.

### Conclusion

We prepared the homogeneous SGDR1 and heterogeneous composite film with SGDR1/GPTS for studying the temporal stability in the second-order NLO effect. Inherent severe decaying behavior of the NLO effect in the sol–gel neat film was much improved using our catalytic silicon precursor (GPTS). The epoxy group in GPTS showed reactivity in the solid state with nucleophilic secondary amine. This gave rise to cross-link formation in the organic side groups. Densification of silicon oxide and the thermal cross-link in organic part have proved to be highly effective in improving the temporal stability of the second-order NLO effect at high temperature.

**Acknowledgment.** This study was supported by the academic research fund of Ministry of Education, Republic of Korea (1996–1997).

CM970311H